Resolving Spatial Resource Gradients at Tidal Energy Sites

Michael T. Palodichuk

A thesis submitted in partial fulfillment
of the requirements for the degree of

Master of Science in Mechanical Engineering

University of Washington

2012

Committee:

Brian Polagye

Jim Thomson

Phil Malte

Program Authorized to Offer Degree: Department of Mechanical Engineering

University of Washington

Abstract

Resolving Spatial Resource Gradients at Tidal Energy Sites

Michael T. Palodichuk

Chair of the Supervisory Committee:
Professor Brian Polagye
Mechanical Engineering

Station-keeping, a vessel-based spatial surveying method for resolving details of the hydrokinetic resource, is presented in the context of the general methodology and also for the specific case of a survey conducted in northern Admiralty Inlet, Puget Sound, WA (USA) in June 2011. The acoustic Doppler current profiler (ADCP) measurements collected during the June 2011 survey were part of a broader effort to characterize the resource at this location prior to tidal turbine installation. Autonomous bottom-lander (bottom-mounted) ADCP measurements are used to evaluate the accuracy with which data collected from this vessel-based survey reflect stationary measurements and also to analyze the potential for cycle-to-cycle variations in the conclusions drawn. Results indicate good agreement between shipboard and bottom-mounted observations in capturing spatial resource gradients. Repeated surveys over several tidal cycles are required to obtain results consistent with long-term observations. Station-keeping surveys help to optimize bottom-mounted ADCP deployments that are then used to estimate turbine power generation potential and make siting decisions.

TABLE OF CONTENTS

LIST OF FIGURES

LIST OF TABLES

ACKNOWLEDGMENTS

I would like to express my sincere appreciation to my committee members, Dr. Brian Polagye, Dr. Jim Thomson, and Dr. Phil Malte, for their continued support and interest. I would especially like to acknowledge my co-advisors, Dr. Brian Polagye and Dr. Jim Thomson, for their help and guidance throughout this project. Their knowledge and passion have truly made this project possible and enjoyable. They have been excellent mentors, and I am extremely grateful.

At the University of Washington Applied Physics Laboratory, I would like to thank Joe Talbert, Alex de Klerk, and Capt. Andy Reay-Ellers for their assistance in collecting these data. I would also like to express my gratitude to all of the faculty and graduate students at the Northwest National Marine Renewable Energy Center for their support. In particular, I would like to recognize Chris Bassett for his help.

I would like to thank my family and friends for their support, inspiration, and interest in my education and research.

My involvement in this project was made possible by funding provided by the United States Department of Energy. Thanks also to Snohomish County Public Utility District for supporting tidal energy in the region.

Chapter 1

PREAMBLE

Tidal hydrokinetic energy is a clean, renewable, and predictable source of energy, wherein free-stream turbines generate power by harnessing the kinetic energy of periodic tidal currents. This resource, while intermittent and variable, is predictable and could be exploited to help alleviate growing energy demands and displace the need for other non-renewable energy sources.

The growing field of marine energy faces unique challenges to its technical and economic viability. Snohomish County Public Utility District is pursuing a tidal energy pilot project in Admiralty Inlet, WA, to learn more about turbine performance and study the potential environmental impacts. If the pilot project is successful, this site has potential to support utility-scale generation. In partnership with the Department of Energy-funded Northwest National Marine Renewable Energy Center (NNMREC) at the University of Washington, a multi-year field study to characterize the physical and biological environment at the project site is being conducted.

In addition to supporting the development of the Admiralty Inlet site, NNMREC aims to establish guidelines for efficient measurement protocols for tidal energy site and device characterization. NNMREC has developed and successfully deployed and recovered multiple autonomous instrumentation packages mounted to bottom-lander tripods (Oceanscience, Ltd. Sea Spiders) in Admiralty Inlet. These bottom-mounted measurements include current velocity (ADCP), water quality (CTDO), underwater noise (hydrophone), and fish and marine mammal presence (fish tag receiver, TPOD and CPOD).

A key component of the studies in Admiralty Inlet is making siting recommendations for the proposed pilot project. Siting decisions will ultimately be made on the basis of resource data collected by these autonomous bottom-mounted ADCP measurements. Vessel-based spatial surveys can, however, provide a complimentary cost-effective means of comparing

relative resource intensity between locations of primary interest. These ship-mounted ADCP surveys can, therefore, optimize the autonomous bottom-mounted ADCP deployments that will be used to estimate turbine power generation potential and make siting decisions.

Admiralty Inlet provides a robust test case for ship-mounted ADCP surveys, and the spatial survey technique demonstrated herein warrants applications to other potential tidal energy sites.

Chapter 2

INTRODUCTION

Tidal hydrokinetic energy is harnessed by free-stream turbines that convert the kinetic energy of strong (> 1 m/s) tidal currents to electricity. Project economics are improved by siting these turbines where the hydrokinetic resource is most energetic. Resource characterization is an early-stage project development activity, with one of the primary objectives being to evaluate the power generation potential for a turbine at a particular location. Site-specific studies indicate that finite-record length observations (minimum 30 days), requiring an autonomous bottom-lander ADCP (acoustic Doppler current profiler), are necessary to estimate long-term turbine power generation potential [12]. Furthermore, siting studies using arrays of autonomous bottom-lander ADCPs have indicated operationally significant variations in the tidal resource (5-10% variations in mean power generation) over length scales less than 100 m, suggesting an economic benefit to micro-siting [12].

Siting turbines within a tidal energy project area, or micro-siting, is discussed in the context of spatial variability on the order of 100 m. Differences in the hydrokinetic resource must be resolved on this scale to inform siting decisions. Surveying over a short time period from a ship-mounted ADCP is economically favorable to a stationary measurement field of ADCPs because of the high execution costs associated with deploying and recovering bottom-lander equipment. In addition to resolving small spatial scale differences, vessel-based surveys must also be designed to minimize uncertainty in the results and minimize cost.

2.1 Literature Review

The potential for ship-mounted ADCP surveys to resolve tidal current gradients was demonstrated by Simpson, et al. [15], where they attempted to detide (i.e., removing tidal currents) observed currents. Repeated transects across a 20 km channel between Scotland and Her-

bides (the Minch) were conducted for approximately one semidiurnal period on two separate cruises and used to map the flow through the Minch. A compound space-time series of measurements at each volumetric bin was built up, and least-squares tidal harmonic analysis was performed to estimate the primary semidiurnal tidal constituents at these discrete points in the profiling transect (1500 m horizontal resolution). The M2 amplitude and phase were in general agreement with a model by Proctor and Wolf [13]. A similar repeated transect methodology was employed by Geyer and Signell [6] to obtain the spatial structure of tidal flow around a headland in Vineyard Sound, Massachusetts. Five 10 km trapezoidal tracks with overlapping edges were surveyed over eight cruises. The semidiurnal amplitude was normalized by moored current meter data, and consistency was shown among the different cruises. The measurements from the separate cruises were merged to form a composite spatial representation of current gradients (up to 500 m horizontal resolution). Vennell [19] applied the method developed by Simpson, et al. to Cook Strait, New Zealand, to determine the horizontal and vertical variation of tidal phase and amplitude within the Strait for a single observed tidal cycle (2500 m horizontal resolution). The measured semi-diurnal tidal amplitude and phase agreed well with a hindcast composite of the three largest tidal constituents from a subsequent one month deployment of bottom-lander ADCPs on the same line as the ship track [21].

For larger spatial scales, Candela, et al. [2] developed a survey methodology that requires only a single survey spanning multiple diurnal periods with no repetitions of any transect. This methodology was applied in the Yellow Sea on a five day cruise over a total survey area of 300 km by 500 km, with horizontal bins segmented 20 km along the ship's track. The primary diurnal and semidiurnal constituents' amplitudes and phases were described as functions of spatial position, and the tidal spatial structure was approximated using arbitrary interpolating base functions. These spatial base functions simulated the horizontal distribution of tidal properties, and their coefficients were set to minimize the residual. Foreman and Freeland [5] followed a similar data collection procedure on a three day cruise around Vancouver Island, Canada, and found that detiding observations using a barotropic numerical model performed better than prescribing spatial base functions.

To demonstrate the physical soundness and consistency of obtained tidal data and sub-

tidal velocity estimates in the mouth of Delaware Bay, USA, Münchow, et al. [10] applied both the repeated transect with harmonic analysis method and the spatial base function method to remove tidal currents, as well as a third method where nearby current meters were used to interpolate tidal currents to the measurement locations. Each discrete station corresponded to a spatial average along the ship track of almost 1000 m, and close agreement of subtidal velocity structure was found among the three methods. Data collection methods similar to the repeated transect method have been employed by Cáceres, et al. [1] in Chacao Channel, Southern Chile and Stevens, et al. [16] in Cook Strait, New Zealand. Vennell and Beatson [20] replaced the volumetric box binning technique with radial basis functions to improve the tidal velocity field extracted from noisy shipboard measurements collected in Bluff Harbour, New Zealand at spatial scales $O(100$ m).

Each of these approaches could conceivably be modified to resolve hydrokinetic resource gradients, but not without difficulty. Most of the techniques involving repeated transects are time intensive for mixed tidal regimes (i.e., survey durations of at least 25 hours), and it is not possible to resolve pure tidal constituents with the limited data collected (i.e., all semidiurnal energy is lumped together into the primary semidiurnal constituent, and all diurnal energy is lumped together into the primary diurnal constituent). Furthermore, the single transect method is restrictive in that it requires either subjectively prescribed spatial base functions (e.g., Candela, et al. [2]) or a validated numerical model of the region under study (e.g., Foremand and Freeland [5]).

For the purposes of micro-siting tidal turbines, Epler, et al. [3] demonstrated a "race-track" method, involving repeated short tracks encompassing a single tidal peak, and applied it in Admiralty Inlet, USA. Data were aggregated within bins such that multiple laps produced time series at 100 m horizontal resolution along the track, with approximately one minute required to transit each bin. The time series was then fitted with a half sine wave, and the amplitude and timing of the peak currents along the survey track were estimated from the fit. Multiple ebb current surveys showed consistency among cycles of differing strength and time of year and were able resolve strong resource gradients (i.e., variations in peak tidal current magnitude greater than 0.3 m/s). Recent turbulence measurements at this site indicate that a one minute temporal mean does not filter the majority of the

turbulent scale motion from the signal [18]. In other words, the effectiveness of the survey technique proposed in Epler, et al. likely depends on implicit turbulence filtering via the half sine wave fit. This approach is generally problematic for locations where the structure of the tidal currents does not conform to a classical harmonic description due to interactions of harmonic currents with bathymetry and topography.

2.2 Overview

A "station-keeping" vessel-based survey methodology is developed in this study to resolve small spatial scale differences in the hydrokinetic resource at low cost. During a station-keeping survey, the vessel occupies each target stations for several, short periods bracketing a single tidal peak. This is unlike the continuous transects of the previous methodologies. Rather than directly comparing the amplitudes of the fits applied to these velocity observations, an energy metric is computed and used to compare the hydrokinetic resource among the surveyed stations.

In this paper, the vessel-based station-keeping methodology is presented and recent results in its applications are described. The data sets and their usage are introduced in Sec. 3.1. They include:

- Shipboard data set: demonstrate the vessel-based station-keeping methodology
- Bottom-mounted data set: ground-truth the effectiveness of a station-keeping survey
- Decimated bottom-mounted data set: analyze the potential for cycle-to-cycle variations in the results of multiple station-keeping surveys

The station-keeping procedure, data processing techniques, and means for station comparison are outlined in Sec. 3.2 through 3.4. Results from the June 2011 station-keeping survey in Admiralty Inlet, USA are then presented in Ch. 4, and the resolution and application of this methodology are discussed in Ch. 5.

Chapter 3

METHODOLOGY

Northern Admiralty Inlet, Puget Sound, WA (USA) is the main entrance to the Puget Sound and is a favorable site for tidal energy development. The tidal exchange through the relative constriction of the channel cross-section gives rise to strong currents. There is currently a proposed hydrokinetic pilot project at this location, undertaken by the Snohomish County Public Utility District, which has the potential to become a utility-scale installation. A multi-year field study has been conducted to broadly characterize the resource prior to tidal turbine installation. Current measurements, collected using Acoustic Doppler current profilers (ADCPs), are a component of these studies. Here, both the general methodology for a station-keeping survey and the specific case for a station-keeping survey conducted in northern Admiralty Inlet are described.

3.1 Data Sets Synopsis

ADCPs use active acoustics to measure currents throughout the water column. In this paper, two types of ADCP data sets are analyzed: those collected from a surface vessel ("shipboard") and those collected from an autonomous bottom lander ("bottom-mounted"). The station-keeping methodology requires only shipboard data. The bottom-mounted data set is used as "truth" to evaluate the accuracy with which data collected from a quasi-stationary surface vessel reflects a stationary measurement and also to mimic multiple station-keeping surveys at the same set of locations.

3.1.1 Shipboard data set

Shipboard surveys are conducted from the University of Washington's Applied Physics Laboratory Research Vessel Jack Robertson (R/V Jack Robertson). Current velocity data is collected using a through-hull Teledyne RDI Workhorse Monitor with instrument configu-

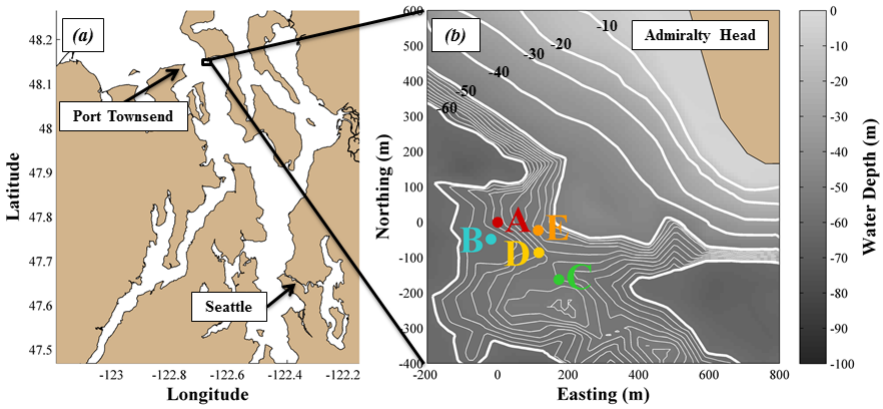

Figure 3.1: Admiralty Inlet tidal energy project area - (a) Regional map. (b) June 2011 station-keeping survey stations overlaying bathymetry (1 m contours are shown for depths between 50 and 60 m).

ration given in Table 3.1. The shipboard ADCP data consist of repeated, short (5 minute) observations during which the vessel occupies a target station. The data collection procedure is explained in detail in Sec. 3.2.

In June, 2011, a station-keeping survey with five target stations was conducted in Admiralty Inlet, Puget Sound. The target stations are summarized in Table 3.2 and shown in Fig. 3.1. Station-keeping targets A, B, and C were selected to be co-spatial with bottom-mounted ADCPs deployed during a prior research cruise. Stations D and E were of potential interest as alternative siting locations for the turbines. Station A is used as a reference location. The June 2011 survey was conducted during an ebb tide in the transitional period between neap and spring tides with peak current velocities around 2 m/s.

3.1.2 Bottom-mounted data set

The objective of this study is to demonstrate the suitability of station-keeping surveys for resolving details of the hydrokinetic resource. Station-keeping is a self-contained shipboard methodology. Bottom-mounted data sets are used here to achieve two objectives. First, they serve to evaluate the accuracy of station-keeping relative to stationary "truth" at survey locations by direct comparison of bottom-mounted and station-keeping time series.

Table 3.1: Shipboard ADCP Configuration

Teledyne RDI Workhorse Monitor	
Acoustic Frequency	307.2 kHz
Time per Ping	0.5 sec
Time between Pings	1 - 2 sec
Vertical Bin Size	4.0 m
Pings / Ensemble	1
Doppler Uncertainty	0.05 m /s
Transducer Depth	1.0 m
Blanking Distance	2.0 m
Motion Compensation	Bottom Tracking

Second, the potential for cycle-to-cycle variations in the conclusions drawn are identified by mimicking multiple station-keeping surveys during different tidal cycles (e.g., spring/neap, ebb/flood, greater/lesser).

As described in Polagye and Thomson [12], bottom-mounted ADCPs were deployed in an upward looking configuration on ballasted fiberglass tripods (Oceanscience Sea Spiders) for periods of up to three months. Details of each deployment are given in Table 3.2 and shown in Fig. 3.1. Bottom-mount Site 1 is a composite record consisting of four deployments, each approximately 3 months in duration from within a 20 m radius. In the context of this study, Site 1 is referred to as the "annual data set."

3.1.3 Decimated data set

Each bottom-mounted ADCP provides long time series observations at a single location. In a station-keeping survey, each station is occupied for several, short periods. For example, in the June 2011 survey, each station was occupied six times for five minutes, with each observation of an individual station separated by 30 to 40 minutes. In order to evaluate the ability of the station-keeping methodology to consistently rank resource intensity between locations, bottom-mounted data is decimated to mimic shipboard data.

Table 3.2: Summary of Survey Stations and Bottom-Mounted ADCP Configurations and Deployments

June 2011 Station-Keeping Survey							
Station	Distance to Station A (m)	Bottom-Mounted ADCP Site (B-M ADCP)	Distance to B-M ADCP (m)	Instrument	Deployment Dates (dd/mm/yy)	Duration (days)	Mean Depth (m)
A	0	1	2	Nortek Continental 470 kHz	18/08/10 - 09/08/11	356	59
B	52	2	16	Nortek AWAC 600 kHz	11/05/11 - 09/08/11	90	61
C	238	3	7	Nortek AWAC 1 MHz	09/05/11 - 08/06/11	30	56
D	145	None	-	-	-	-	-
E	117	None	-	-	-	-	-

To create these data sets, the bottom-mounted ADCP data is first averaged to five minute ensembles and separated into individual ebb or flood cycles. The five minute average filters the majority of the turbulent motion from the record [18]. To simulate a survey pattern, six sequential ensembles, each separated by 35 minutes, are selected. By incrementing the starting time for each survey, each decimated bottom-mounted data set yields twenty survey realizations per tidal cycle (cycle duration and timing restrictions are discussed in Sec. 3.2). Additionally, only cycles with current amplitude greater than 1 m/s are retained (as also discussed in Sec. 3.2). The collection of realizations for all tidal cycles meeting the decimation analysis criteria (cycle duration, timing restrictions, current amplitude) is referred to as the "decimated data set." Each tidal cycle in the decimated data set is categorized by the direction (flood/ebb), diurnal inequality (greater/lesser), and fortnightly variation (spring/neap).

Observations are presented at 22 m elevation relative to the seabed throughout this paper. This was selected because it is an elevation where shipboard and bottom-mounted observations overlap, is within the range of hub heights for first generation tidal turbines, and is outside the region of strongest vertical shear.

3.2 Procedure and Parameter Selection for a Station-Keeping Survey

Station-keeping surveys are performed during tidal cycles having peak current amplitudes of at least 1 m/s, and observations are collected around the time of peak currents since these provide the strongest signal for resolving spatial gradients and also represent the period of maximum power output from a hydrokinetic tidal turbine (kinetic resource intensity varies with the cube of velocity). During a station-keeping survey, the survey vessel sequentially occupies the target stations to obtain a sparse time series for each station, ideally with an equal number of observations on both sides of peak currents.

The following survey parameters are recommended to maximize the quality of data collected. Observation timing, tidal conditions during the survey, temporal resolution, and spatial resolution are all important.

3.2.1 Observation Timing

The number and relative locations of the target stations influence the number of observations that can be collected per station and the temporal spacing between these observations. In the June 2011 station-keeping survey, five target stations were sequentially occupied to obtain six observations per station, with these observations separated by approximately 35 minutes. As discussed in Sec. 3.3, the error associated with a station-keeping survey is minimized with at least five observations per station and 30-40 minutes time separation between each observation. Variations in observation timing relative to peak currents also influence this error (as also discussed in Sec 3.3), which is further minimized with an equal number of observations on each side of peak currents. This may require that the timing of peak currents be known to high accuracy, and realizations with an unequal number of observations on each side of peak currents are considered (i.e., the difference between the number of observations collected prior to peak currents and the number of observation collected after peak currents is two or less).

For individual tidal cycles in the decimated data sets, variations in observation timing relative to peak currents are simulated by incrementing the starting time for each survey. Mimicking the June 2011 survey pattern with six sequential ensembles, each separated by 35 minutes, yields twenty unique survey realizations per tidal cycle that contain at least two observations on each side of peak currents. To obtain these twenty realizations, tidal cycles must be at least 4.5 hours in duration. Similarly, peak currents must occur at least 2.25 hours after and prior to slack water.

3.2.2 Tidal Conditions

Applying the decimation analysis criteria (cycle duration, timing restrictions, current amplitude) to the annual data set provides insight into the tidal conditions in which station-keeping surveys are effective. Tidal cycles that pass the criteria allow sufficient time for the survey to be conducted (with some flexibility in survey start time relative to peak currents) and provide strong signal for resolving spatial gradients. The tidal conditions analyzed are flood/ebb (direction), greater/lesser (diurnal inequality), and spring/neap (fortnightly

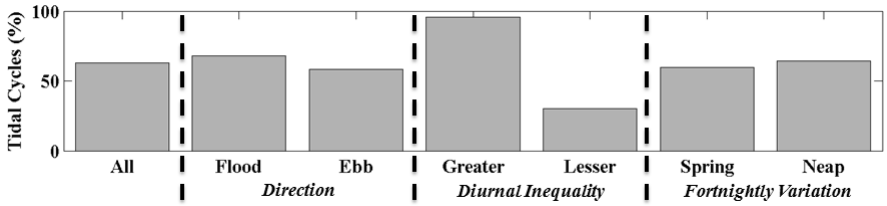

Figure 3.2: Decimation analysis on tidal conditions - Percentages of tidal cycles passing the decimation analysis criteria for each tidal condition.

variation). Note that the diurnal inequality is a feature of mixed tidal regimes, such occur in northern Admiralty Inlet and along most of the west coast of the United States. For each tidal cycle, the pass/fail criteria for inclusion in the decimated data set is defined as a cycle duration of at least 4.5 hours, with 2.25 hours separating peak currents from either bounding slack event, and minimum peak amplitude of 1 m/s. A comparison of the pass rates for the categories of tidal conditions in Admiralty Inlet is shown in Fig. 3.2. Of the 1345 tidal cycles observed by the bottom-mounted ADCP, 849 pass the above criteria.

Whether an individual tidal cycle passes the analysis criteria is primarily influenced by diurnal inequality, and appears to be independent of the direction and fortnightly variation. The duration of the lesser tides of the diurnal inequality, are often too short or low intensity for a station-keeping survey. These results suggest that in locations of mixed tidal regimes, the effectiveness of station-keeping surveys is improved when they are performed during greater tides, which provide strong signal and enough time for all six observations to be collected.

3.2.3 Temporal Resolution

The duration of each station occupation is set to capture only information about the deterministic component of the currents by averaging out variability associated with Doppler noise and turbulent fluctuations. As seen in (3.1), a single ADCP ping (u_{meas}) reflects not only the deterministic tidal forcing (u_{det}) and meteorological component (u_{met}), but also turbulence fluctuations (u_{turb}) and the Doppler noise from the instrument (η_{samp}). As stated in Polagye and Thomson [12], the deterministic currents include harmonic currents,

described by harmonic constituents [7, 4], as well as the aharmonic response to these currents induced by local topography and bathymetry. Aharmonic currents are not described by tidal constituents, but are repeatable, site-specific flow features [11]. Meteorological currents include wave- and wind-induced motion [22, 9], residual currents associated with estuarine stratification [8], and storm surges [14]. Turbulent currents include large-scale, horizontal eddies and small-scale, isotropic turbulence [18]. The relative contribution of these elements to measured currents is site-specific.

$$u_{meas} = u_{det} + u_{met} + u_{turb} \pm n_{samp} \tag{3.1}$$

To reduce the Doppler noise inherent to single-ping ADCP data, the data are aggregated into a series of volumetric bins. A certain number of samples are necessary in each bin to achieve some standard of normal statistics and the noise must be reduced, but the number of samples must be such that the deterministic and meteorological currents are statistically stationary and the vertical extent of each sample bin must be spatial homogeneous.

A vertical bin size of 4.0 m has been selected for this application because it results in an acceptably low Doppler uncertainty per ping (0.05 m/s) and still provides information at a resolution sufficient for siting decisions. The implicit assumption of spatial homogeneity over the depth bins should, however, be viewed with some caution, especially near the seabed where the velocity profile changes significantly with depth due to the influence of the boundary layer (Polagye and Thomson [12] provides further discussion on this point).

A canonical value for turbulence intensity over all stages of the tide (i.e., the turbulent velocity fluctuations relative to the mean tidal currents) is 10% [18]. Strong currents at potential tidal energy sites, including northern Admiralty Inlet, can exceed 3 m/s. It is assumed that both the Doppler noise and turbulence fluctuations are normally distributed about the mean, deterministic currents.

Reducing the contribution from turbulence and Doppler noise to the measured current velocity requires a minimum number of sample pings per station occupation. The minimum sample size is determined using confidence intervals for a nonstandard normal distribution (3.2) and comparing them to the interval set by the desired precision (3.3). Here u is

the estimated population mean, u_{true} is the true population mean (unknown), u_{obs} is the sample mean (ensemble-average), Z is the normal inverse cumulative distribution, α is the confidence level, s is the sample standard deviation, N is sample size, and p is the desired precision.

$$u = u_{obs} \pm Z_{\alpha/2}\frac{s}{\sqrt{N}} \tag{3.2}$$

$$u = u_{true} \pm p \tag{3.3}$$

The minimum number of required samples that yield the desired precision is determined by an estimate for the standard deviation (i.e., both Doppler noise and turbulence) and a confidence level. In other words, with the standard deviation set by Doppler noise and turbulence velocity fluctuations, and the normal inverse cumulative distribution set by the confidence level, the number of samples on the right-hand side of (3.2) is chosen, such that the ensemble-average velocity confidence interval is less than or equal to the desired precision for the true velocity on the right-hand side of (3.3). To determine, *a priori*, the minimum number of samples required for the June 2011 station-keeping survey in Admiralty Inlet, the Doppler uncertainty is modeled as ±0.05 m/s (Table 3.1), and the turbulence velocity fluctuations are modeled as ±0.30 m/s (10% of 3 m/s velocity). The relation between precision and sample size is shown in Fig. 3.3.

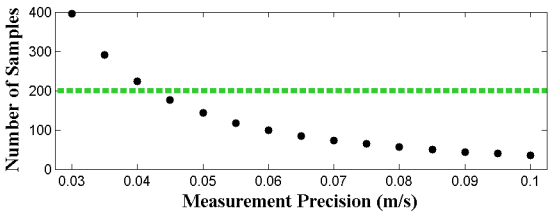

Figure 3.3: Sample size requirements for the June 2011 survey - Normal statistics with 95% confidence for Doppler uncertainty in Table 3.1 and turbulence consistent with observations from Admiralty Inlet. Green dashed line denotes the number of samples from a 5 minute observation receiving good pings every 1-2 seconds.

Greater precision requires increasing the number of samples per ensemble interval. In a

useful station-keeping survey, it is desired that the measurement precision be significantly less than the spatial resource variations that are of operational interest for a site developer. For the June 2011 survey, the desired precision was on the order of 0.10 m/s (i.e., higher precision than could be obtained by the survey methodology described in Epler, et al. [3]). At least 143 samples per ensemble interval are required to obtain 0.05 m/s precision. With the configuration shown in Table 3.1, the ADCP receives a good ping every 1-2 s and five minute ensembles yield better than 0.05 m/s precision. In Thomson, et al. [18], five minute ensembles are empirically determined to be the longest duration with a stable mean and variance (i.e., stationary statistics) that do not require detrending to account for non-stationarity in the deterministic currents, while windows shorter than five minutes tend to include a portion of the turbulent currents.

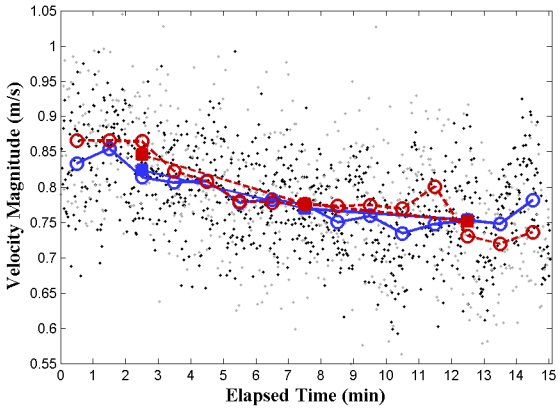

Figure 3.4: Shipboard and bottom-mounted ADCP velocity observations - Raw and ensemble-averaged observations at 22 m elevation relative to seabed at Station C. Black dots denote bottom-mounted pings, and grey dots denote shipboard pings. Bottom-mounted ensembles (blue) are connected by solid lines, and shipboard ensembles (red) are connected by dashed lines. Circles denote 1 minute ensemble intervals, and squares denote 5 minute ensemble intervals.

To confirm the observation duration was sufficient to achieve the desired precision, a single extended observation was conducted at Station C prior to the start of the June 2011 survey. As shown in Fig. 3.4, the observations from the shipboard ADCP are ensembled over different intervals and compared to co-temporal and co-spatial bottom-mounted data.

The five minute ensemble interval captures the trend in the deterministic components of the current magnitude, with minimal fluctuations. In addition, over this interval, the difference between shipboard observations and bottom-mounted "truth" is small in comparison with the desired precision.

3.2.4 Spatial Resolution

For the June 2011 survey, the 50 m tolerance radius around the target station for the vessel was selected *a posteriori* as this was the minimum tolerance that could be achieved by the R/V Jack Robertson's captain in strong and variable currents. Vessels equipped with dynamic positioning systems may be able to achieve tighter tolerances.

Differential Global Position System (DGPS) coordinate location (converted to relative easting, x, and northing, y, with respect to the reference station) is recorded for each ADCP ping (GPS mast is almost directly above the ADCP wet well). For the series of observations at an individual station, the target location becomes the mean of the ping locations, rather than the original target location, to better characterize the accuracy of the collected data. The track error (δ_{track}) is computed as the mean distance from the ping locations to mean survey position. The coordinate error associated with the use of a DGPS (δ_{DGPS}) is minimal and assumed to be no more than 5 meters. This error could be significant if a station-keeping survey was to be conducted without a DGPS.

ADCP beam spread is defined as $\delta_{beam} = 2d\tan(\theta)$, where θ is the transducer mounting angle from vertical and d is the vertical distance between the transducer head and sample bin. For a shipboard measurement, beam spreading is small near the surface and it is reasonable to assume that spatial homogeneity is achieved between the beams (four beams in this specific case). As shown in Fig. 3.5, this assumption becomes more tenuous at greater depths, particularly when attempting to resolve small spatial scales. The cross-section of the horizontal area being surveyed is considered the beam spread error.

The track, DGPS, and beam spread errors are uncorrelated and can be combined using (3.4) in order to obtain a total position error, δ_r, with respect to the target station. In order for observations between two stations to be statistically independent, the position

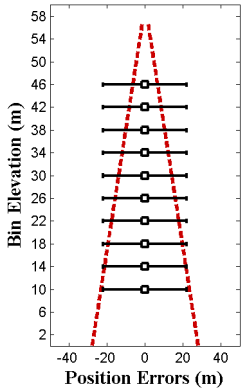

Figure 3.5: Position errors throughout the water column - Horizontal bars denote the vessel's typical track error over the target station, and red dashed lines denote beam spread of the shipboard ADCP.

ambiguities (i.e., target location $\pm\delta_r$) cannot overlap. Independence between two stations is tested by (3.5).

$$\delta_r = \sqrt{\delta_{track}^2 + \delta_{DGPS}^2 + \delta_{beam}^2} \tag{3.4}$$

$$\sqrt{(x_1 - x_2)^2 + (y_1 - y_2)^2} - \delta_{r1} - \delta_{r2} > 0 \tag{3.5}$$

3.3 Data Processing

Bottom tracking is used to remove ship motion from ADCP measured water velocities. Several factors determine whether or not an individual ping will be successfully received and processed by the ADCP, with the ship speed being the most important. Ship speeds below 3.0 m/s combined with minimal pitch and roll allow sufficient time for the ADCP to receive the bottom track. Given that station-keeping vessel velocities are very low, this is rarely a problem.

Hard returns from the seafloor contaminate measurements in the lowest bins. Measured values not meeting a minimum correlation count are removed. Any measurements from outside of the tolerance radius for a target station are discarded. The quality assured data

is then processed in the following steps.

3.3.1 Ensemble-Average Velocity

The representative ensemble-average current velocity for each observation (u_{obs}) is calculated for each depth bin using (3.6). The population mean and standard deviation of each observation is unknown and must be estimated from the sample mean and standard deviation. There are sufficient pings per ensemble to assume a normal statistical distribution for turbulent perturbations and Doppler noise.

$$\begin{aligned} u_{obs} = \overline{u_{meas}} &= \overline{u_{det} + u_{met} + u_{turb} \pm n_{samp}} \\ &\approx u_{det} + u_{met} \pm n_{ens} \end{aligned} \tag{3.6}$$

The temporal mean filters the majority of the turbulent scale motion from the signal [18], while preserving the deterministic and meteorological components [12]. The Doppler noise (η_{ens}) is reduced by a factor of $N^{1/2}$ relative to the original Doppler noise (η_{samp}), where N is the number of samples in the ensemble.

3.3.2 Kinetic Power Density

Kinetic power density (K) is computed for each velocity observation as

$$K = \frac{1}{2}\rho u_{obs}^3 \tag{3.7}$$

where ρ is density (assumed to be 1024 kg/m3). This is not identical to the average of the kinetic power density for each ping in the ensemble (i.e., the mean of the cube is not equal to the cube of the mean). Doppler noise and turbulence intensity, assumed to have zero mean values and defined by their second moments, do not bias the mean velocity. However, if K is computed directly from each ping, the result will be biased high by the symmetric variance in these systems. To avoid asystematic error in kinetic power density computation from Doppler noise, the best unbiased velocity value is used (i.e., the ensemble

mean). Based on analysis of high-resolution bottom-mounted data, the difference between using $\overline{u_{meas}}^3$ and $\overline{u_{meas}^3}$ is minimal over the five-minute time scale (not shown).

Because measurements of kinetic power density are sparse in a station-keeping survey and are obtained at each station at different times relative to the peak currents, a representation of resource intensity is required that is insensitive to potential variations in tidal phase between locations. Therefore, an empirical fit is developed to describe observations for each station. The analysis is conducted in Matlab (www.mathworks.com) using the default unconstrained nonlinear optimization routine. Three types of empirical fits were considered. The first is a polynomial fit

$$\widetilde{K}(t) = x_0 + x_1 t + ... x_n t^n \tag{3.8}$$

where $\widetilde{K}$ is the empirical fit to the observations of K and x are the polynomial coefficients. The second is a modified polynomial fit where the coefficients are determined by bottom-mounted ADCP data obtained simultaneously with the shipboard data at one location within the survey area. This is a hybrid survey technique combining aspects of shipboard and bottom-mounted surveys methodology. An amplitude correction factor and time offset become the free parameters being fit at each station and depth. This enables the use of higher-order polynomials to describe the time-variation in K. The third is a sinusoid fit

$$\widetilde{K}(t) = \frac{1}{2}\rho(A\sin(\omega t + \phi))^3 \tag{3.9}$$

where A is the current velocity amplitude, ω is the tidal frequency, and ϕ is the relative phase. While this fit has some justification on the basis of harmonic analysis, measured tidal currents at tidal energy sites rarely resemble a smoothly varying sinusoid [11]. These various fits were applied to all tidal cycle realizations of the decimated data set to benchmark their relative effectiveness. A comparison of how the fits represent the data is shown in Fig. 3.6, and the quality of the various fits is discussed as it pertains to the kinetic energy density.

3.3.3 Kinetic Energy Density

The kinetic energy density (KE) is obtained by numerically integrating $\widetilde{K}$ over a two hour period during peak kinetic power density using a cumulative trapezoidal method. This is used to provide an estimate for relative resource intensity differences between stations that is insensitive to the times at which the stations are occupied. The starting time for the two hour period is chosen iteratively to maximize KE for each station from observational data (or realization in the decimated data set). The two hour period is a reasonable choice for the integration window. Testing with other windows indicates that periods less than two hours or greater than three hours tend to introduce a systematic error in the computation of the KE.

The KE associated with each of the potential curve fits is calculated for all tidal cycle realizations in the decimated data set ($N = 849$ tidal cycles with 20 realizations per cycle). An estimate for the "true" KE for each tidal cycle is computed by numerically integrating the undecimated observations of K using a cumulative trapezoidal method. The relative error (ϵ) for each realization is evaluated using (3.10). For each of the fit types, a standard relative error (σ_ϵ) is defined as the standard deviation of the relative errors for all realizations. A comparison of the quality of fits is shown in Fig. 3.6.

$$\epsilon = \frac{KE_{obs} - KE_{true}}{KE_{obs}} \tag{3.10}$$

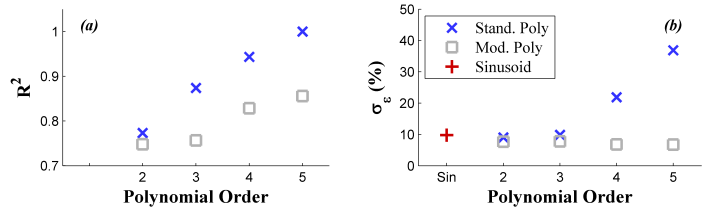

Figure 3.6: Quality of fits to K - (a) Goodness of fit to observed data. Note that the sinusoid fit is not shown because R^2 value is not comparable to the other fits (i.e., for the sinusoid fit, the fit is applied to the velocity ensembles and the result is then cubed, whereas for the 2^{nd} order polynomial fit, the fit is applied directly to the kinetic power density). (b) Quality of fit in calculating KE. Both analyses performed at 22 m elevation relative to seabed.

For the basic polynomial fits, increasing the order of the polynomial improves the coefficient of determination. However, higher order fits are prone to buckling and do not necessarily represent the underlying structure of the data accurately. This is evident in the high relative errors associated with the 5^{th} order fit (even though the coefficient of determination is highest). The 2^{nd} order polynomial and sinusoid descriptions of the kinetic energy density perform nearly as well as all orders of the modified polynomial informed by bottom-mounted data. The minimal improvement gained by using bottom-mounted data to inform the fitting is not justifiable because of the high execution cost to deploy and recover autonomous bottom-lander equipment simultaneously with shipboard surveys. A comparison between the 2^{nd} order polynomial and sinusoid descriptions indicate that they perform similarly throughout the water column (not shown). The effectiveness of these fits is further tested in the context of the observation parameters.

Again using the kinetic energy density metric and the standard relative error in its computation, modifications to the baseline observation parameters (i.e., six observations per station with temporal spacing of 35 minutes) are considered using the decimated data set. The objective is to choose a number of observations and time between observations, as well as a fitting method, that minimizes σ_ϵ. From the decimated data set, 849 tidal cycles are analyzed. The number of realizations per tidal cycle depends on the observations parameters being analyzed (i.e. number of observations and temporal spacing between observations). For all realizations of the station-keeping surveys scenarios analyzed, the difference between the number of observations collected prior to peak currents and the number of observation collected after peak currents is never greater than two. The standard relative error for each scenario is found as the mean of the relative errors for all realizations. Results of this analysis are shown in Fig. 3.7.

The 2^{nd} order polynomial and sinusoid fits again perform similarly for sampling intervals around the baseline parameters (i.e., six observations separated by 35 minutes). In scenarios nearing the limits of the variations applied to the observation parameters, the 2^{nd} order fit appears to be more accurate. Particularly for the scenario of 4 observations in Fig. 3.7(a) the σ_ϵ value is approximately 63% for the sinusoid fit (not shown) and only 20% for the 2^{nd} order polynomial fit. The 2^{nd} order polynomial fit proves to be more robust in representing

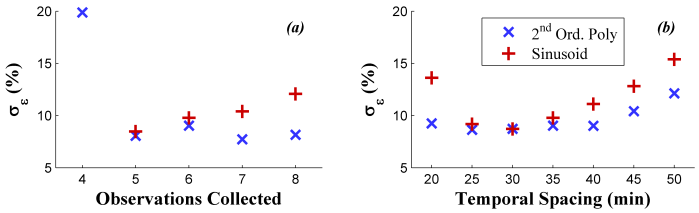

Figure 3.7: Effects of varying survey parameters on computation of KE - (a) Effect of varying number of observations collected with time between observations held constant at 35 minutes. (b) Effect of varying time between observations with number of observations held constant at six. Both analyses performed at 22 m elevation relative to the seabed.

the underlying data with variations to these observation parameters. As such, it is used to represent the resource intensity.

Furthermore, these results demonstrate that collecting at least five observations per station substantially decreases the standard relative error in the computation of the KE. The temporal spacing between observations also influences the computation of the KE. The two hour KE value bracketing peak currents is of primary interest, and smaller spacing (e.g., 20-25 min) between observations can result in a better estimate of the KE because of the higher resolution during this window. High σ_ϵ can, however, result from such a station-keeping survey if there are an unequal number of observations on each side of peak currents (not shown) because one of the ends of the window is not bounded by an observation. Larger spacing (e.g. 45-50 min) results in lower resolution around peak currents, provides less flexibility in survey start time, and increases the overall duration of the survey. Collecting observations with temporal spacing of 30-40 minutes provides sufficient resolution bracketing peak currents, does not necessitate an equal number of observations on each side of peak currents, and allows flexibility in survey start time. Therefore, the recommended survey strategy is to bracket peak currents at all stations and occupy each station at least five times, with each occupation separated by 30-40 minutes.

The effect of starting time relative to peak currents is also evaluated using the standard error. The standard relative error for each survey start time shown in Fig. 3.8 is computed as the mean of the relative errors of that set of realizations. Realizations with start times

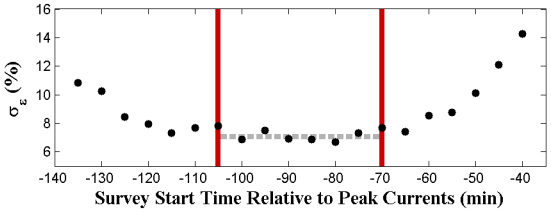

Figure 3.8: KE standard error based on survey start time relative to peak currents - Black dots denote standard relative error for each survey start time. Red solid lines denote conservative start time bounds for which an equal number of observations are collected on either side of peak (6 stations, 35 minute separation between observations at each station). Grey dashed line denotes the standard relative error for survey start times within these bounds. Analyses performed at 22 m elevation relative to seabed.

that include an equal number of observations on both sides of the peak have the smallest relative errors. This indicates that the effectiveness of a station-keeping survey is improved when the survey starts approximately 70-105 minutes prior to the timing of peak currents. Given that the timing of peak currents may not be known to high accuracy (or may vary by more than 60 minutes between the surface and seabed) before the survey is initiated, conservative start times are indicated. Assuming that the survey begins as discussed, the standard relative error is calculated as the mean of all realizations meeting this criteria.

Fig. 3.9 shows the distribution of relative errors for one vertical bin and the standard relative error throughout the water column. The distribution of these errors has a nearly zero mean value indicating that the data processing techniques do not bias the computation of the KE. As discussed in Sec. 3.2, the station-keeping survey methodology can be improved by surveying during greater tidal cycles, which is demonstrated in the comparison of the standard relative error values between all tidal cycles and greater tidal cycles (Fig. 3.9(b)). Velocity varies less smoothly in time near the seabed due to the influence of bottom effects (bottom friction and local acceleration due to bathymetry). The standard error, as calculated relative to the undecimated observations of K, increases near the seabed. We suspect that this is a data processing artifact; the fitting technique is not sensitive to these variations.

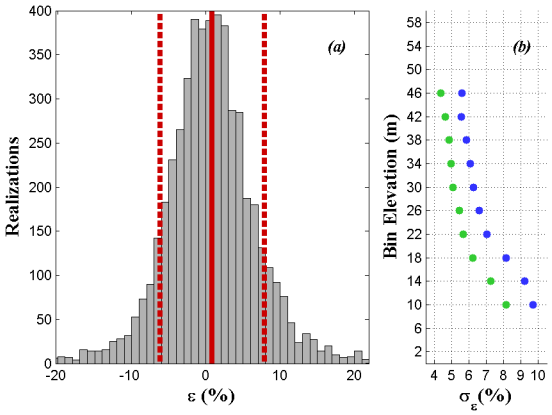

Figure 3.9: KE relative error for conservative start times - (a) Distribution of error at 22 m elevation relative to seabed. Red solid line denotes mean value, and red dashed lines denote one standard deviation from the mean value. Three standard deviations from the mean value of the distribution are shown. (b) KE standard relative error throughout water column. Blue dots denote the standard relative error for all tidal cycles, and green dots denote the standard relative error for greater tidal cycles.

3.4 Kinetic Energy Density Normalization

The hydrokinetic resource may be compared between two stations by normalizing their KE values to a reference, denoted by superscript "0" (3.11). The relative error associated with the ratio of two KE values is the additive combination of their individual standard relative errors, as in equation (3.12) [17]. Here, σ_ϵ is the relative error for a desired confidence interval.

$$KE_{obs}^{1/0} = \frac{KE_{obs}^{1}}{KE_{obs}^{0}} \tag{3.11}$$

$$KE_{true}^{1/0} = \frac{KE_{obs}^{1}(1 \pm \sigma_\epsilon)}{KE_{obs}^{0}(1 \pm \sigma_\epsilon)} = KE_{obs}^{1/0}(1 \pm 2\sigma_\epsilon) \tag{3.12}$$

Chapter 4

RESULTS

In June, 2011, a station-keeping survey with five stations (A-E, shown in Fig. 3.1) was conducted near Admiralty Head in Admiralty Inlet, Puget Sound. Each station was occupied six times for five minutes, with each observation of an individual station separated by 30 to 40 minutes. The survey was conducted during a lesser ebb tide in the transitional period of the neap-spring cycle with peak current velocities around 2 m/s. During this transitional period of the neap-spring cycle, greater and lesser tides are nearly equal in strength.

4.1 Station Comparison

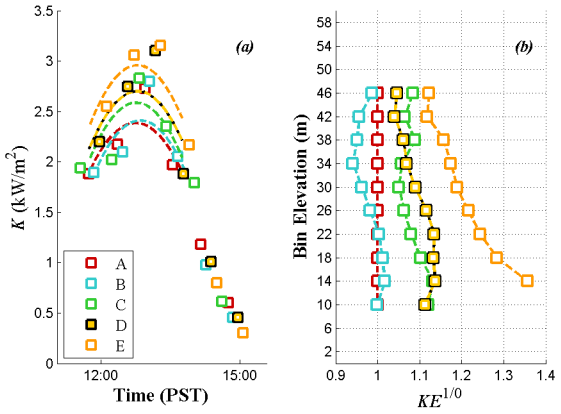

Figure 4.1: Comparison of the hydrokinetic resource among target stations - (a) Polynomial curve fits through observed K at 22 m elevation relative to seabed. (b) Normalized KE values with respect to Station A. Note that one of the six observations at Station E contained contaminated data in the bottommost (10 m) bin - this data is not shown.

The data collected from the shipboard ADCP is processed as described in Sec. 3.3 (e.g., 2^{nd} order polynomial fit), and the kinetic energy density calculated over a two hour window.

The hydrokinetic resource is compared among stations in Fig. 4.1, with Station A used as the reference station.

These results suggest that Stations C, D, and E are the most energetic. This is especially evident in the lower bins where the relative KE is more than 10% higher at these target stations.

4.2 Methodology Evaluation

Stations A, B, and C were chosen because these were co-spatial with bottom-mounted ADCPs, allowing us to ground-truth the effectiveness of the station-keeping survey methodology. A comparison of shipboard and bottom-mounted observations is shown in Fig. 4.2.

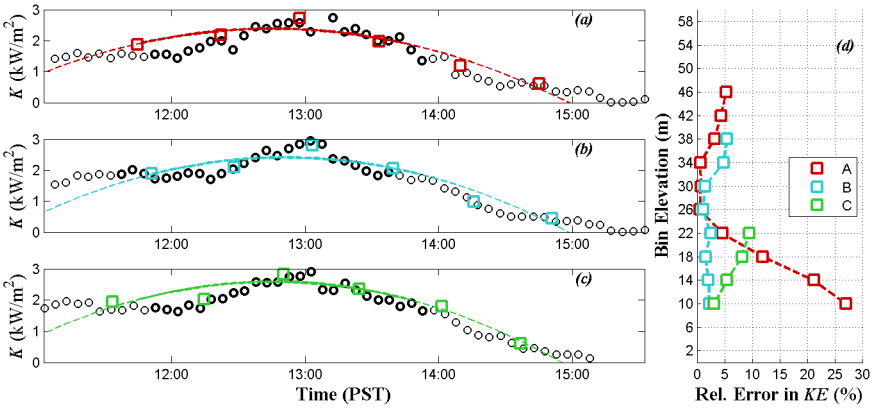

Figure 4.2: Shipboard and bottom-mounted observations of K and KE - (a-c) Comparison of observed K at 22 m elevation for Stations A-C (co-spatial with Sites 1-3), respectively. Circles denote bottom-mounted ensembles, with the bolded circles used to compute the "true" KE. The dashed line denotes the fit to the shipboard ensemble (squares), with the bolded portion used to compute the "observed" KE. (d) Relative error between the observed and true KE. Note that the comparison is only possible for common vertical bins between the two instruments: the upward looking ADCPs have a maximum range set by their configurations and the downward looking ADCP signal is contaminated by the hard return from the seabed in the lower two bins.

These results indicate good agreement between the shipboard and bottom-mounted observations. The error associated with KE values obtained in the upper half of the water column is within the expected error (σ_ϵ, Fig. 3.9). All bins of Stations B and C are also

Table 4.1: Normalized Kinetic Energy Densities

June 2011 Station-Keeping Survey, 22 m Elevation		
Station	$KE^{1/0}$	
	Shipboard ("obs") [1]	Bottom-Mounted ("true")
A ("0")	1.00 ± 0.14	1.00
B	1.00 ± 0.14	1.02
C	1.08 ± 0.15	1.03
D	1.13 ± 0.16	-
E	1.24 ± 0.17	-

[1] Standard error based on analysis of decimated data set (Fig. 3.9)

within this expected error. The discrepancy in the observations in the lower bins at Station A is due to an instrumentation configuration problem with the bottom-mounted ADCP[1].

The normalized KE values ($KE^{1/0}$) for each station are shown in Table 4.1. Note that this table is comparing the results of the station-keeping methodology as observed to the true values for this tidal cycle. It is not a comparison of the error between bottom-mounted and shipboard data for each individual station. In other words, $KE^{1/0}$ for the shipboard data are referenced to the shipboard results for Station A, $KE^{1/0}$ for the bottom-mounted data are referenced to the bottom-mounted results for Site 1 (co-spatial with Station A).

[1]The distance between pings (equivalent to the time delay) was insufficient to avoid interference between the incoming and outgoing pulse in these bins. The along-beam distance of approximately 132 m ($2 * 60/\cos(25^\circ) = 132$ m in 60 m depth) was greater than the lag of 120 m by 12 m, and thus the surface reflection would be getting back about 12 m above the instrument when the next ping went out. Analysis of the along-beam velocities indicate destructive interference, with all three along-beam velocities going to near-zero in these bins (not shown). This would explain the consistent overestimation in current velocity observations of the shipboard ADCP relative to the bottom-mounted ADCP at Station A at these elevations (not shown).

Chapter 5

DISCUSSION

5.1 Impact of Positions Errors

Target stations need to be sufficiently separated in space for observations to be statistically independent. This separation is governed by the positioning errors in the survey, namely the beam spread of the ADCP, the track error of the vessel, and the DGPS error. Statistical independence between observations of two stations is tested by (3.5).

From the June 2011 station-keeping survey, the beam spread was approximately 31 m at a bin elevation of 22 m, and the track error was approximately 22 m for each station. From (4), this yields a total position error of 38 m associated with each station. Consequently, Station B was not statistically independent from the reference (Station A), as the locations were only separated by 52 m and their combined total position errors were 76 m (i.e., spatial overlap of 24 m). Of the pings collected during observations over these stations, approximately 20% overlapped with the station not being surveyed.

The resolution of the station-keeping methodology is limited by these positioning errors. The total position error defines the resolution radius associated with each station (i.e., the resolution is twice the total position error). Choosing target stations such that they are separated by at least twice the expected total position error improves survey effectiveness. Note that beam spread is a function of depth, so it is possible for the observations from two stations to be statistically independent near the surface and not statistically independent at lower elevations relative to the seabed. Furthermore, tighter tolerances in the vessel's track about the target station reduce the spatial ambiguity and increase the resolution of a station-keeping survey.

5.2 Survey Application

During the June 2011 station-keeping survey, Station A and Station C each had a co-spatial bottom-mounted ADCP (Site 1 and Site 3, respectively). These bottom-mounted ADCPs were simultaneously deployed at their respective locations for 30 days, from May to June 2011. For resource metrics related to performance, reasonable accuracy is obtained from 30-day observations [12].

To mimic multiple station-keeping surveys at these locations, the true normalized KE value and an observed normalized KE value were computed from the decimated data sets. The "true" value for normalized KE (i.e., $KE_{true}^{C/A}$) for each tidal cycle is computed from the complete set of KE ensembles over the two hour integration window. The corresponding observed value (i.e., $KE_{obs}^{C/A}$) is calculated from the decimated realization from that cycle with survey start time 90 minutes prior to peak currents. A comparison of these $KE^{C/A}$ values is shown in Fig. 5.1.

The 30 day data set is separated into 107 tidal cycles, of which 48 greater tidal cycles meet the decimation analysis criteria (Sec. 3.2). Of the 48 greater tidal cycles, 47 of $KE_{true}^{C/A}$ fall within the 68% confidence interval of $KE_{obs}^{C/A}$, and 48 of the true values fell within the 95% confidence interval of the observed values (not shown). As found in the June 2011 station-keeping survey, these results suggest that Station C is, in general, more energetic than Station A (see Fig. 4.1).

Although the station-keeping methodology generally performs well for a single tidal cycle (x's and squares compare well in Fig. 5.1(b)), the observed spatial resource gradients vary with tidal cycle (i.e., the observed gradients over a single survey may not accurately represent the true long-term average gradients). Multiple station-keeping surveys over the same target stations can be conducted to increase the confidence that observed values reflect the true, long-term values.

The normalized KE metric, computed from a single station-keeping survey, is used to compare the hydrokinetic resource between target stations. As described in Polagye and Thomson [12], metrics calculated from finite-length observations may diverge from their true values (defined as the average over an infinite observation). The convergence of the

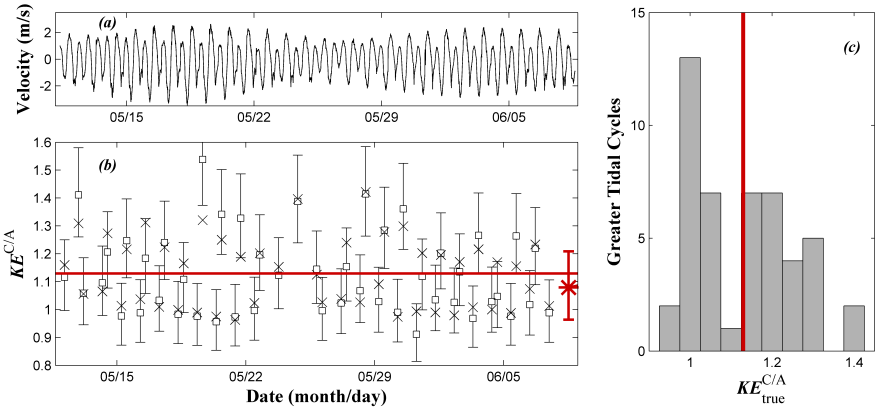

Figure 5.1: Normalized KE values over multiple tidal cycles - Observations at 22 m elevation relative to the seabed (a) Velocity observations at Station C from bottom-mounted ADCP data (b) Normalized KE values (Station C referenced to Station A) - x's denote "true" values. Squares denote observed values, with the error bars bounding the 68% confidence interval (set by the standard error (see Fig. 3.9)). Red horizontal line denotes the mean of the 48 true values, and the red star denotes the observed value during the June 2011 station-keeping survey. (c) Histogram of true normalized KE values. Red vertical line denotes the mean of the 48 true values.

normalized KE metric to its true value is given by

$$\frac{\int_0^S KE^{C/A}(s)ds \,/\, \int_0^S ds}{\int_0^\infty KE^{C/A}(s)ds \,/\, \int_0^\infty ds} \tag{5.1}$$

where $KE^{C/A}(s)$ is the observation varying normalized KE metric and S is the number of consecutive surveys on greater tides. In shorthand, the averaging number of observations is represented with a superscript and positions are said to have converged when $(KE^{C/A})^S \approx (KE^{C/A})^\infty$. Since $(KE^{C/A})^\infty$ is not known *a priori*, this convergence can only be investigated in a proximate manner. The true normalized KE average of the greater tidal cycles over an infinite number of observation $(KE^{C/A})^\infty$ is approximated by the mean of the true normalized KE values obtained from the 48 greater tidal cycles over the 30 days of mimicked station-keeping observations $(KE^{C/A})^{48}$. Multiple 48-cycle realizations are created by generating a ring buffer from the 30 day data set. Fig. 5.2 shows the convergence of the normalized KE (Station C referenced to Station A), to its 48-observation mean value.

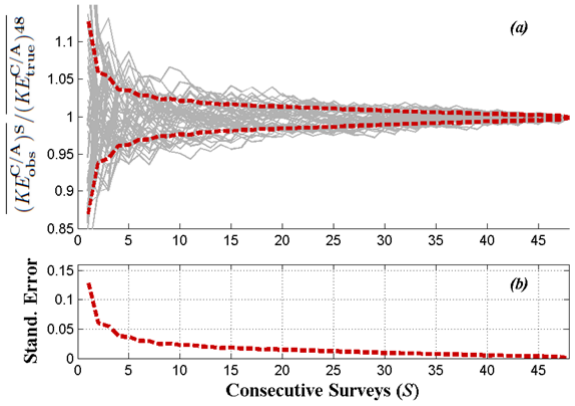

Figure 5.2: Convergence of normalized KE to its long-term average - (a) Convergence to 48-observation mean value. Thin grey lines denote individual realizations over the 30 day period. Red dashed lines denote standard error. (b) Standard error normalized by running mean normalized kinetic energy density as a function of observation time.

The normalized standard error relative to the long-term average decreases to less than 5% after four surveys on consecutive greater tidal cycles meeting the decimation analysis criteria (cycle duration, timing restrictions, current amplitude, as discussed in Sec. 3.2). The standard error then continues a gradual decay. Provided that data collection is performed as suggested in Ch. 3 (e.g., an equal number of observations to either side of peak currents is ideal), convergence trends are not markedly different for variations in survey start time relative to peak currents. For the purposes of characterizing differences in the hydrokinetic resource between two locations, a record length of four consecutive surveys on greater tidal cycles provides 5% accuracy. Additional surveys may be necessary if an individual greater tidal cycle does not allow sufficient time for the survey to be conducted or does not provide strong signal for resolving spatial gradients (i.e., it does not pass the decimation analysis criteria). The standard error for a single survey can approach 20%, which may be unacceptably high for optimizing subsequent deployment of a bottom-lander to estimate turbine power generation.

A comparable metric to the KE for characterizing differences in the hydrokinetic resources from current velocity observations of bottom mounted ADCPs is the mean kinetic

Table 5.1: Comparison of KE and $\overline{K}$

Station	Station-Keeping		Bottom-Mounted Deployments [1]	
	$\overline{(KE^{1/0})^S}$ [2]	S (consecutive surveys)	$\overline{(\overline{K}^{1/0})^T}$ [3]	T (deployment duration)
A ("0")	1.00 ± 0.04	4	1.00 ± 0.04	356
C	1.13 ± 0.04	4	1.13 ± 0.08	30

[1] Bottom-mounted deployments are co-spatial with station-keeping targets (Table 3.2)

[2] Standard error with respect to 48-observation mean value (Fig. 5.1)

[3] Standard error with respect to its epoch value based on analysis of harmonic velocity [12]

power density – the time average of the kinetic power density – given by

$$\overline{K} = \overline{\frac{1}{2}\rho u_{obs}^3} \tag{5.2}$$

Following from Polagye and Thomson [12], this resource characteristic is computed for the bottom-mounted ADCP deployments at Sites 1 and 3 (co-spatial with Stations A and C, respectively). The comparison of the normalized KE values ($KE^{1/0}$) from multiple station-keeping surveys (mimicked using the decimated data) and the normalized $\overline{K}$ values ($\overline{K}^{1/0}$) from the complete bottom-mounted data is shown in Table 5.1. Note that 4-observation mean $KE^{1/0}$ is equal to the 48-observation mean $KE^{1/0}$ because of the ring buffer data structure.

The objective of the station-keeping methodology is to resolve relative gradiations in the hydrokinetic resource. This vessel-based methodology, and the normalized KE metric, captures the same spatial trends as those developed from multiple, high-cost bottom-mounted deployments with similar accuracy, provided that the station-keeping survey is repeated at least four times on consecutive greater tidal cycles that provide sufficient time for the survey to be conducted and provide strong signal for resolving spatial gradients.

Chapter 6

CONCLUSIONS

This methodology is suitable for resolving small spatial scale differences and minimizing uncertainty in results. The desired spatial resolution of 100 m or less is achieved by selecting stations such that their spatial ambiguities do not overlap, and the resolution could be further improved by tighter tolerances in the vessel's track about the target station. Uncertainty in the results is minimized by determining a minimum duration of each station occupation that will capture only information about the deterministic component of the currents.

Analysis of a yearlong bottom-mounted ADCP data set indicates the most effective tidal conditions to conduct the survey, determines optimal observation timing and spacing, and reduces the potential for data processing artifacts (i.e., sensitivity to type of fit). Bottom-mounted data sets were also used as "truth" to evaluate the accuracy of the methodology and its effectiveness. Results indicate good agreement between shipboard and bottom-mounted observations in capturing spatial trends of the hydrokinetic resource over a single tidal peak. Multiple, consecutive observations during greater tidal cycles can be used to characterize resource gradients with certainty approaching long-term (i.e., 30 day) bottom-mounted deployments.

Station-keeping is an effective and economically favorable alternative to generating siting data from a high-resolution grid of bottom-mounted ADCPs.

Chapter 7

POSTSCRIPT

Minimizing cost is a primary factor in the application of data collection techniques for the purposes of generating siting data. A grid of bottom-mounted ADCPs provides simultaneous stationary measurements with low uncertainty, but as demonstrated in Sec. 5.2, performing the vessel-based station-keeping methodology during multiple, consecutive greater tidal cycles captures the same spatial trends as those characterized by this bottom-mounted grid. A simple cost analysis between multiple shipboard ADCP surveys and a grid of bottom-mounted ADCPs is used to compare the relative economics of these approaches.

In this cost analysis, the two techniques are applied to characterize difference in the hydrokinetic resource among five stations. Tidal cycle duration, the relative locations of the stations, and the survey parameters impose a limit to the number of target stations that can be selected for a single station-keeping survey. A five station survey is generally achievable. It is possible to scale this technique to incorporate a larger number of stations using multiple survey vessels simultaneously with a common reference station.

The R/V Jack Robertson is used in this analysis as the vessel for the shipboard ADCP surveys, as well as the vessel for the deployment and recovery operations of the bottom-mounted ADCP packages. This vessel is equipped with the equipment and instruments necessary for station-keeping surveys (i.e., thru-hull ADCP) and deployment/recovery operations (i.e., A-frame, winch, weight bearing acoustic release, command/ranging deck unit). Furthermore, it is assumed that the fully burdened day rate of $3,000 for the R/V Jack Robertson (personal communication, J. Thomson, University of Washington Applied Physics Laboratory) includes the cost of employing the captain and technicians.

Station-keeping surveys are performed twice per day (on greater ebb and greater flood) at the specified day rate for the R/V Jack Robertson. This technique does not have a base cost and has a constant variable cost for up to five stations.

Table 7.1: Bottom-Mounted ADCP Instrument Package Costs

Instrument/Equipment	Base Cost ($/Unit)	Day Rate ($/Unit)	Units per Package
ADCP(w/ battery pack)	300	110	1
Frame	30	10	1
Ballast	800 [1]	-	1
Acoustic Release	240	25	2
Float	30	10	2
Total (per Station)	1670	190	-

[1] Personal communication, J. Thomson, University of Washington Applied Physics Laboratory. This information was not listed by Orders Associates Research Systems, LLC.

Rental costs (base cost and day rate) for the bottom-mounted ADCPs were collected from Orders Associates Research Systems, LLC (www.oarsllc.com) and are detailed in Table 7.1. Bottom-mounted ADCPs are deployed in an upward looking configuration on ballasted frames. These instrument packages are autonomous–powered by battery packs–and require two redundant acoustic releases connected to floats and retrieval lines. Deployment and recovery operations can only take place around slack water, and the number of instrument packages that can be deployed or recovered per slack is dependent on slack duration and tidal conditions. Deploying or recovering five instrument packages would likely require at least two slack waters, and a day of ship time has been allocated on each end of deployment for this purpose. As show in Table 7.2, the grid of bottom-mounted ADCPs has a base cost of $6,000 for deployment and recovery ($\$3,000 * 2 = \$6,000$ for two days of ship time) plus the base instrument package cost of $1670 per station. The day rate of $190 per instrument package also scales with the number of stations.

Fig. 7.1 shows the cost-per-day analysis of the two techniques for characterizing the differences in the hydrokinetic resource among five stations. The cost of the two techniques intersects at seven days, indicating that performing multiple station-keeping surveys is more cost-effective for observation records of less than seven days.

Table 7.2: Five Station Bottom-Mounted ADCP Grid Costs

Expense	Base Cost ($)	Day Rate ($)
Instrument Packages	8350	950
Recovery and Deployment	6000	-
Total	14350	950

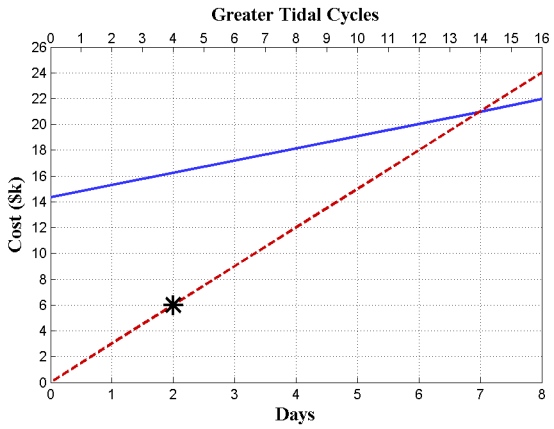

Figure 7.1: Cost analysis for characterizing differences in the hydrokinetic resource among five stations - Red dashed line denotes per-day-cost of shipboard ADCP surveys, and blue solid line denotes per-day-cost of a grid of bottom-mounted ADCPs. Star denotes a record length of four consecutive station-keeping surveys on greater tidal cycles (over two days).

A record length of four consecutive station-keeping surveys on greater tidal cycles (indicated by the star in the Fig. 7.1) provides 5% accuracy in computing the normalized KE metric for station comparison (Fig. 5.2). Additional surveys may be necessary if an individual greater tidal cycle does not allow sufficient time for the survey to be conducted or does not provide strong signal for resolving spatial gradients. For observations records of two days (containing four greater tidal cycles), a grid of bottom-mounted ADCPs costs over twice that of performing the vessel-based station-keeping methodology during the greater tidal cycles over that period. These results demonstrate the economic favorability of using the station-keeping methodology for characterizing resource gradients for the purpose of generating siting data. Once spatial resource gradients have been established, a long-term

(i.e., 30 day) bottom deployment will be necessary to more fully characterize the turbine deployment location (e.g., quantification of turbulence, long-term kinetic power density, directional variability).

BIBLIOGRAPHY

[1] M. Cáceres, A. Valle-Levinson, and L. Atkinson. Observations of cross-channel structure of flow in an energetic tidal channel. *J. Geophys. Res.*, 108(C4):1–10, April 2003.

[2] J. Candela, R.C. Beardsley, and R. Limeburner. Removing tides from ship-mounted adcp data, with application to the Yellow Sea. In *Current Measurement, 1990., Proceedings of the IEEE Fourth Working Conference on*, pages 258–266, April 1990.

[3] J. Epler, B. Polagye, and J. Thomson. Shipboard acoustic doppler current profiler surveys to assess tidal current resources. In *OCEANS 2010*, pages 1–10, September 2010.

[4] M.G.G. Foreman, R.F. Crawford, and W.R. Marsden. De-tiding: theory and practice. *Quantitative Skill Assessment for Coastal Ocean Models, Coastal and Estuarine Studies*, 47:203–239, 1995.

[5] M.G.G. Foreman and H.J. Freeland. A comparison of techniques for tide removal from ship-mounted acoustic Doppler measurements along the southwest coast of Vancouver Island. *J. Geophys. Res.*, 96(C9):17007–17021, 1991.

[6] W.R. Geyer and R. Signell. Measurements of tidal flow around a headland with a shipboard acoustic Doppler current profiler. *J. Geophys. Res.*, 95(C3):3189–3197, 1990.

[7] G. Godin. On the predictability of currents. *International Hydrographic Review*, 60:119–126, 1983.

[8] D.V. Hansen and M. Rattray. *Gravitational circulation in straits and estuaries.* Technical report (University of Washington. Dept. of Oceanography). Sears Foundation for Marine Research, 1965.

[9] C.C. Mei. *The applied dynamics of ocean surface waves.* Advanced series on ocean engineering. World Scientific, 1989.

[10] A. Münchow, R.W. Garvine, and T.F. Pfeiffer. Subtidal currents from a shipboard acoustic Doppler current profiler in tidally dominated waters. *Continental Shelf Research*, 12(4):499–515, 1992.

[11] B. Polagye, J. Epler, and J. Thomson. Limits to the predictability of tidal current energy. In *OCEANS 2010*, pages 1–9, September 2010.

[12] B. Polagye and J. Thomson. Tidal energy resource characterization: methodology and field study in Admiralty Inlet, Puget Sound, US. *Submitted*.

[13] R. Proctor and J. Wolfe. An investigation of the storm surge of the storm surge of 1st February 1983 using numerical models. *Focus on modelling marine systems*, 1, 1990.

[14] D.T. Pugh. *Tides, surges, and mean sea-level*. J. Wiley, 1987.

[15] J.H. Simpson, E.G. Mitchelson-Jacob, and A.E. Hill. Flow structure in a channel from an acoustic Doppler current profiler. *Continental Shelf Research*, 10(6):589–603, 1990.

[16] C.L. Stevens, M.J. Smith, B. Grant, C.L. Stewart, and T. Divett. Tidal energy resource complexity in a large strait: The Karori rip, Cook Strait. *Continental Shelf Research*, 33:100–109, 2012.

[17] J.R. Taylor. *An introduction to error analysis: the study of uncertainties in physical measurements*. Series of books in physics. University Science Books, 1982.

[18] J. Thomson, B. Polagye, V. Durgesh, and M. Richmond. Measurements of turbulence at two tidal energy sites in Puget Sound, WA (USA). *J. Ocean. Eng., In press*.

[19] R. Vennell. Acoustic Doppler current profiler measurements of tidal phase and amplitude in Cook Strait, New Zealand. *Continental Shelf Research*, 14(4):353–364, 1994.

[20] R. Vennell and R. Beatson. Moving vessel acoustic Doppler current profiler measurement of tidal stream function using radial basis functions. *J. Geophys. Res.*, 111(C9):1–15, September 2006.

[21] R. Vennell and N. Collins. Acoustic Doppler current profiler measurements of tides in Cook Strait, New Zealand. *Coastal Engineering-Climate for Change. Proceedings of 10th Australasian Conference on Coastal and Ocean Engineering*, (21):529–534, 1991.

[22] D. Wang. Wind-driven circulation in the Chesapeake Bay, winter, 1975. *J. Phys. Oceanogr.*, 9(3):564–572, May 1979.